JOURNAL OF CATALYSIS 31, 346–359 (1973)

Mössbauer Spectroscopy of CO Shift Catalysts Promoted with Lead

H. TOPSØE AND M. BOUDART*

Stauffer Laboratories of Chemistry and Chemical Engineering,
Stanford University, California 94305

Received February 12, 1973

Lead promotes the activity of Cr-promoted magnetite CO shift catalysts. An analysis of the Mössbauer parameters of the Pb-promoted catalysts shows that lead enters the spinel structure as Pb^{4+} on tetrahedral sites, giving rise to a partly normal spinel structure. Attempts to synthesize the Pb^{4+}-containing Fe–Cr spinel by firing the oxides in vacuum at 1000°C failed, indicating Pb^{4+} is not stable in the spinel structure at high temperature. In fact it exsolves from the Pb-promoted catalyst upon heating to above 700°C. The data indicate that the octahedral Fe^{3+} ions exhibit an increased covalency as a result of promotion by lead. This together with the inherent defect structure of the spinel phase may explain the enhanced activity toward the CO shift reaction at 400°C.

INTRODUCTION

Ferrites are widely used as catalysts and magnetic materials. This study deals with the structure of promoted magnetite catalysts for the conversion of CO with steam to H_2 and CO_2, called the CO shift reaction. The conventional catalyst for the CO shift reaction is based on iron oxide-chromium oxide (*1*). The stable iron oxide under reaction conditions is Fe_3O_4, with a spinel structure which is probably the active part of the catalyst as chromium acts mainly as a textual promoter to prevent sintering.

Recently Topsøe (*2*) and Bohlbro (*3*) reported that PbO added to an iron oxide–chromium oxide catalyst increased the catalytic activity per unit surface area for the CO shift reaction. In the present paper we examine how lead could affect the structure of the catalyst. Magnetite has a spinel structure with the oxygen ions forming a face-centered cubic close-packed lattice. In this lattice, the cations are placed in tetrahedral *A* sites and octahedral *B* sites, with a unit cell written as $(Fe_8{}^{3+})_A[Fe_8{}^{3+}Fe_8{}^{2+}]_BO_{32}$. If the trivalent ions are distributed equally between the *A* and *B* sites, the spinel is said to be inverse. When all the trivalent ions are located on the *B* sites, the spinel is designated as normal. Intermediate structures between the normal and inverse spinel are also found. Magnetite is a ferrimagnet with spins of the cations ordered parallel within each *A* and *B* sublattice.

Gorter has determined that only metallic ions with Goldschmidt radii r between 0.44 and 1.0 Å can form cubic spinels (*4*). Recently Ca^{2+} ($r = 1.06$ Å) has been reported to enter the magnetite lattice, but solid solutions exist only with small concentrations of Ca, and at higher concentrations of Ca, a separate orthorhombic phase appears (*4–7*). It would thus appear very unlikely that Pb^{2+} with an ionic radius of 1.32 Å could dissolve in magnetite. By contrast, chromium which is added to the catalyst as a textural promoter enters the magnetite lattice as Cr^{3+} on the *B* sites (*8*).

The Mössbauer spectrum of Fe_3O_4 shows two magnetically split 6-line patterns above 119 K, where the spectrum with the larger hyperfine field is due to Fe^{3+} in the *A* sites. The spectrum with the smaller hyperfine

---

* To whom correspondence should be addressed.

field arises from the Fe^{2+} and Fe^{3+} ions in the B site. Above 119 K there is a fast electronic exchange (hopping) between the B site ions so that only one magnetically split B pattern arises. The ratio S of the B spectral area to the A spectral area is close to 2 above 119 K, since the number of atoms responsible for the B spectrum is twice the number of atoms responsible for the A spectrum. The B ions are ordered magnetically below 119 K resulting in a complex Mössbauer pattern. The ratio Fe^{3+}/Fe^{2+} is denoted by R and is equal to 2 in stoichiometric magnetite. Robbins *et al.* (*9*) have extensively studied the Mössbauer characteristics of magnetite–chromite systems. Several hexogonal structures (also called hexagonal ferrites) of the general formula $PbO \cdot xFe_2O_3$ have been reported, with the Pb^{2+} ions replacing oxygen ions ($r = 1.32$ Å) (*8*). The Mössbauer spectrum of these types of compounds shows significant differences from that of magnetite (*10*).

EXPERIMENTAL

Sample Preparation

Magnetite catalysts contained 5% Cr, 7% Cr, and 5% Cr + 5% Pb (all percentages as atomic based on cations). The first and last samples will be designated as Cr–Fe_3O_4 and CrPb–Fe_3O_4. Samples were prepared as follows (*2*). A solution of ferrosulfate was first converted into a precipitate of ferrooxalate consisting of coarse crystals from which impurities were easily removed, resulting in a low sulfur content in the final catalyst. An equivalent amount of NaOH was added to the pure ferrous oxalate suspension, and after the mixture had been kept at 368 K for 1 hr the ultrapure $Fe(OH)_2$ was filtered and washed. Chromic acid was then added, and the mixture was heated to 373 K for ½ hr. In the case of the lead-containing catalysts, this step was followed by an addition of lead nitrate, and finally the precipitate was filtered and dried. Unless otherwise specified, the catalysts studied were used for 1 yr at 673 K, 1 atm, with a gas composition of 50% H_2O, 30% H_2, 10% N_2, 5% CO, and 5% CO_2. Some catalysts were sintered in a CO–CO_2 mixture containing 6.1% CO at 1040 K for 16 hr.

Spinels were made in our laboratory by firing stoichiometric amounts of powdered Fe, Fe_2O_3, and promoter oxide(s), mixed in an agate mortar, in a Pt boat inside an evacuated (2×10^{-5} Torr), and sealed quartz tube. The samples were heated to 1270 K for 12 hr and cooled to room temperature at a rate of 0.1 K s^{-1}. The reagents were Fe_2O_3 (99.999%, A. D. Mackay), Fe (99.999%, Johnson Mathey), PbO (99.999%, Johnson Mathey), PbO_2 (95%, Baker and Adamson), CaO (Mallinkrodt Analytical Reagent), and Cr_2O_3 (Baker and Adamson). The Cr_2O_3 was first heated to 670 K in air, and the Fe_2O_3 used for preparing Fe_3O_4 by reaction with a CO–CO_2 mixture at 703 K was a Baker and Adamson analytical reagent containing less than 0.2 wt% foreign cations. The preparation of the Fe–MgO catalysts has been described elsewhere (*11*).

For chemical analysis of samples, Fe^{3+} was determined by dissolving the catalyst in HCl under an atmosphere of CO_2 and N_2 and then titrating under N_2 with EDTA using salicyclic acid as an indicator at pH 4. Total iron was determined by the same method after dissolving the sample in hot HCl + HNO_3, and lead was determined by solution in HNO_3 to determine the sulfate gravimetrically. Chromium was assayed photometrically with EDTA and Si was determined by atomic absorption.

Samples of the catalysts which had first been evacuated at 440 K were heated to 700–750 K in the presence of a known amount of O_2 until no further uptake was noticed in a gas volumetric system.

Mössbauer Spectroscopy

The spectrometer is described elsewhere (*12, 13*). A typical spectrum of a 1 mil Fe foil at 297 ± 2 K showed parameters (*13*) in excellent agreement with the NBS values at 297 ± 0.5 K (*14*). The hyperfine parameters for magnetite type Mössbauer spectra were obtained from a constrained computer fit which took into account the relaxation broadening of the B spectra (*13*).

The absorber was prepared from a mixture of the catalyst and inert diluent Linde 13 X molecular sieve. The diluent produced stable wafers with small density of ^{57}Fe atoms (less than 5×10^{18} ^{57}Fe atoms cm^{-2}). The absorber was mounted in transmission geometry in variable temperature cells, spanning the temperature region 10–1000 K while maintaining a vacuum or a controlled atmosphere (*13*, *15*).

X Ray Diffraction

A Picker biplanar diffractometer was used to obtain the X ray diffraction patterns. The samples were mounted in powder form on Plexiglass sample holders which eliminated interfering peaks but showed a somewhat large background at low diffraction angles. The radiation was Mo K_α, and a solid state detector was employed. The digital output was computer fitted. In the cases where accurate d values were required, powder from a Si single crystal was mixed with the sample as an internal standard. A polycrystalline quartz sample was used to correct for instrumental broadening in particle size determinations. The particle size was calculated from the Scherrer equation correcting for both instrumental broadening, and $K_{\alpha 1}$ and $K_{\alpha 2}$ doublet (*13*, *16*).

RESULTS

X Ray Diffraction and Particle Size Results

The X ray diffraction patterns of the Cr–Fe_3O_4 (Fig. 1a) and the CrPb–Fe_3O_4 (Fig. 1b) catalysts both showed the presence of the magnetic diffraction pattern. The relative intensities of the diffraction lines were, within experimental error, equal to those observed for a pure Fe_3O_4 sample. Repeated experiments with a Si internal standard present showed that the lattice constant for catalysts containing lead was about 0.015 Å larger than for samples containing only Cr, the latter being around 8.392 Å, in quite good agreement with the expected value for Cr–Fe_3O_4 (*9*). The X ray diffraction pattern (Fig. 1b) of the lead-containing catalyst showed some faint peaks (d values in Å = 1.865, ~3.50, ~3.60, 2.83), not belonging to the magnetite diffraction pattern, which could be attributed to a small amount of free lead oxide or lead chromate. From X ray line broadening, the characteristic dimension of the CrPb–Fe_3O_4 particles was found to be 370 Å.

The X ray diffraction pattern of the sintered CrPb–Fe_3O_4 catalyst showed be-

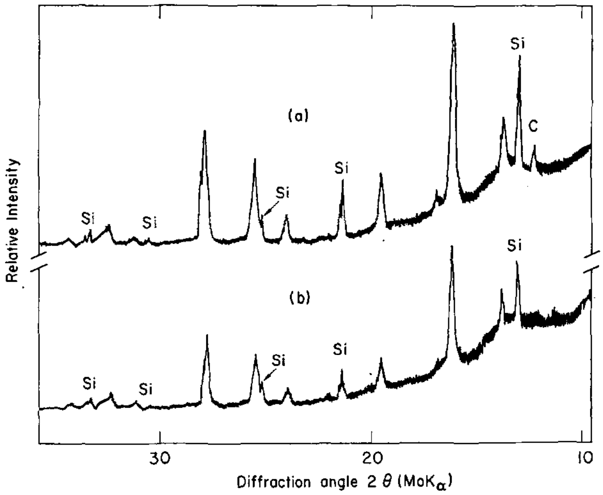

FIG. 1. X ray diffraction patterns, taken with Si as an internal standard of samples exposed to air: (a) Cr/Fe_3O_4; (b) CrPb–Fe_3O_4.

sides a magnetite diffraction pattern also several strong new diffraction lines; the strongest ones were $d = 2.859$ ($I/I_{311} = 19$, I_{311} being the intensity of the (311) diffraction line of Fe_3O_4), $d = 3.357$ ($I/I_{311} = 8$), $d = 1.495$ ($I/I_{311} = 5$) and $d = 2.479$ ($I/I_{311} = 4$). All the new diffraction lines could be attributed to separate Pb or PbO phases. X ray line broadening on the two samples showed that the size of the sintered CrPb–Fe_3O_4 sample was ≥ 800 Å.

X ray diffraction patterns of the Cr–Fe_3O_4 catalyst (7% Cr) used for oxidation experiments showed that after the last oxidation at 750 K for 7 hr, the catalyst consisted of γ-Fe_2O_3 of which about 30% was converted to α-Fe_2O_3. The diffraction pattern of the oxidized CrPb–Fe_3O_4 catalyst showed that even after oxidation at about 750 K for 32 hr, no trace of α-Fe_2O_3 was present, and the phase showed only the γ-Fe_2O_3 diffraction pattern.

The 36% Fe–MgO catalyst has been described elsewhere (*11*). After reduction with H_2, it contained Fe^{2+} in solid solution with MgO as well as metallic iron particles with a size of 200 Å as determined by CO chemisorption and X ray line broadening. Thus, when these iron particles of this catalyst were converted into magnetite, their particle size was ca. 250 Å.

Chemical Analysis and Oxidation

It is possible that the concentration of promoters in the catalyst changes after long exposure under reaction conditions and chemical analyses of the samples were therefore performed. Analyses of Fe^{3+} and total iron were also carried out to check for deviations in the stoichiometric ratio $R = Fe^{3+}/Fe^{2+}$, and results are listed in Table 1. Chemical analysis of samples sintered in quartz tubes showed no contamination of the catalysts by Si. Results from oxidation experiments are also listed in Table 1. The oxidation was done at two temperatures. Values for the Cr–Fe_3O_4 catalyst (7% Cr) were calculated on the assumption that the catalyst was a stoichiometric spinel in which a fraction of the Fe^{2+} ions was oxidized to Fe^{3+} according to the symbolic representation

$$3Fe^{2+} \rightarrow 2Fe^{3+} + \square \qquad (1)$$

where $\square$ is a vacancy. We can thus write the structure of the catalyst after oxidation as:

$$Fe^{2+}{}_{1-3\gamma}Fe^{3+}{}_{2+2\gamma-x}Cr_x{}^{3+}\square_\gamma O_4. \qquad (2)$$

No assumption has been made about the detailed distribution of cations and vacancies on the *A* and *B* sublattice.

For the lead-containing catalyst *R* depends on the assumed valence for lead which is assumed to enter the structure given by formula (2). Table 1 shows *R* for three situations: R_2 and R_1 corresponding to Pb^{2+} replacement of Fe^{2+} with and without complete oxidation to Pb^{4+}, respectively, and R_3 corresponding to Pb^{4+} present in the structure according to the symbolic representation

$$2Fe^{3+} \rightarrow Fe^{2+} + Pb^{4+}. \qquad (3)$$

TABLE 1

CHEMICAL ANALYSIS OF USED AND OXIDIZED CATALYSTS[a]

	Used		Oxidized	
	Cr^{3+}	Pb	Conditions	*R*
7% Cr–Fe_3O_4	6.94	—	16 hr at 430°C followed by 7 hr at 480°C	3.02
CrPb–Fe_3O_4	4.77	4.93	24 hr at 460°C followed by 32 hr at 480°C	$R_1 = 4.70$ $R_2 = 16.3$ $R_3 = 4.57$

[a] Cation composition in atm %; $R = Fe^{3+}/Fe^{2+}$; R_1, R_2, R_3 defined in text.

Mössbauer Spectroscopy

Mössbauer spectra were recorded at several temperatures in a controlled atmosphere following reduction of the samples in a 4:1 CO_2–CO mixture at 703 K. To check the reduction and to obtain a Fe_3O_4 standard, a sample of pure α-Fe_2O_3 was first reduced, and spectra were recorded at different temperatures (Fig. 2). The computer-fitted values for the spectral parameters are listed in Table 2. Although some of the values for the individual parameters may be questionable, erroneous conclusions drawn from bad values are less likely to be reached when the whole temperature range behavior is considered. The Mössbauer parameters at room temperature agree with those reported in the literature (*9, 17–20*) thus, the reduction gives stoichiometric magnetite. The temperature dependence of the magnetic fields agrees well with those obtained by Van der Woude *et al.* (*21*). A small quadrupole splitting seems to be present in both spectral components, in agreement with the recent data of Dobson *et al.* (*20*).

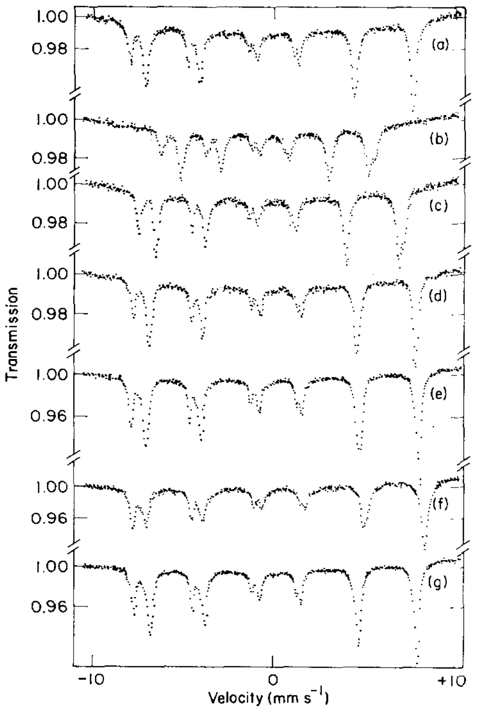

FIG. 2. Mössbauer spectra of Fe_3O_4 (Mössbauer spectra have been plotted without background correction). (a) Fe_2O_3 reduced in a $CO_2/CO = 4$ mixture at 703 K for 13 hr. Spectrum obtained in reaction mixture at 296 K. (b) After further reduction of (a) for 6 hr at similar condition. Spectrum obtained in reaction mixture at 703 K. (c) After cooling (b) to 483 K. (d) After cooling (c) to 296 K. (e) After heating (f) to 208 K. (f) Cooling (d) to 111 K in He (2 Torr). (g) After heating (e) to 296 K.

The experiments at temperatures below room temperature were carried out under He atmosphere in a liquid nitrogen Mössbauer cell. A room temperature Mössbauer spectrum (Fig. 2g) was produced after the low temperature measurements and showed that no oxidation had occurred during the transfer to the liquid nitrogen dewar. The spectrum at 111 K shows that the ordering of the octahedral ions has started, but the typical spectrum of magnetite below T_{Verwey} (*22*) has not yet been obtained.

The Mössbauer spectra of the Cr–Fe_3O_4 catalyst are shown in Fig. 3, and the hyperfine parameters are given in Table 2. The spectrum before (Fig. 3a) and after (Fig. 3d) the reduction shows significant differences, and, furthermore, the spectrum changed during exposure to air at room temperature (see Fig. 4 and (*13*)).

The Mössbauer spectra of the CrPb–Fe_3O_4 catalyst before and after treatment with a CO_2–CO = 4 mixture at 703 K are shown in Fig. 4. The computer-fitted spectral parameters are given in Table 2. The Mössbauer spectrum at room temperature after the reduction (Fig. 4d) was identical to the Mössbauer spectrum after long exposure to air (Fig. 4a). An additional reduction (Fig. 4e) did not result in further changes. The spectral parameters did not change after exposure to air at room temperature (Fig. 5).

The spectra of the catalyst containing lead show many obvious features which are very different from the spectra of pure Fe_3O_4 and the catalyst containing only chromium. The most striking difference is the very large value of the area ratio S ($S = A_{1B}/A_{1A}$). At increasing temperatures, we observed an increased fraction of a paramagnetic doublet (at 297 K: $QS =$

TABLE 2

PARAMETERS OF MÖSSBAUER SPECTRA OBTAINED BETWEEN 111 AND 703 K UNDER CONTROLLED ATMOSPHERE[a]

Sample	T (K)	A_{1B} / A_{1A}	H_A (kOe)	H_B (kOe)	$\delta_{A,\mathrm{Fe}}$ (mm s^{-1})	$\delta_{B,\mathrm{Fe}}$ (mm s^{-1})	$4\epsilon_A$ (mm s^{-1})	$4\epsilon_B$ (mm s^{-1})	Γ_{1A} (mm s^{-1})	Γ_{1B} (mm s^{-1})
Fe_3O_4	703	1.81	368.4	322.9	0.050	0.422	0.028	0.010	0.376	0.371
	483	1.44	459.9	419.1	0.181	0.551	0.057	0.102	0.337	0.305
	296	1.87	490.8	460.9	0.258	0.670	−0.111	0.186	0.349	0.392
	111	1.25	504.9	483.8	0.341	0.770	−0.036	0.124	0.383	0.516
CrPb–Fe_3O_4	703	5.0	327	291	0.12	0.40	0.17	−0.22	0.40	1.77
	483	4.2	448.7	404.6	0.161	0.550	0.183	0.031	0.301	0.916
	296	4.0	487.3	449.2	0.285	0.639	−0.010	0.006	0.309	0.848
	119	4.1	503.1	478.8	0.358	0.688	−0.013	0.104	0.349	1.338
Cr–Fe_3O_4	703	2.26	356.9	308.1	0.064	0.420	0.014	0.062	0.524	0.588
	483	1.54	458.6	419.8	0.192	0.541	0.080	0.097	0.428	0.425
	296	1.63	489.2	456.9	0.274	0.644	−0.054	0.197	0.386	0.461
36% Fe_3O_4–MgO	703	2.79	351.6	312.4	0.052	0.400	0.126	0.040	0.786	0.849
	483	2.60	452.0	416.5	0.195	0.534	0.138	0.108	0.370	0.676
	296	2.02	485.7	455.4	0.270	0.629	−0.033	0.069	0.428	0.776

[a] Subscripts A and B denote A and B spectrum, respectively; subscripts $1A$ and $1B$ denote line $1A$ and $1B$ of the Fe_3O_4-like spectrum; δ_{Fe} is the isomer shift with respect to Fe; ϵ is the splitting of each of the excited levels due to quadrupole interaction; $\epsilon = (V_6 - V_5 - V_2 + V_1)/4$; Γ is the line width (full-width of half-maximum).

0.403 mm s^{-1}, $\delta_{\mathrm{Fe}} = 0.330$ mm s^{-1}). From computer fit of the inner region we can estimate that, at about 720 K, 50% of the total spectral area results from the paramagnetic component. At 703 K, the magnetically hyperfine split component of the spectrum is not well defined, and the usefulness of many of the computer-fitted parameters is limited.

The Mössbauer spectra of the 250 Å Fe_3O_4 particles in the 36% Fe_3O_4–MgO catalyst are shown in Fig. 6. The results from the computer fit are listed in Table 2. Around 820 K, the area of a paramagnetic component equals that of the magnetically hyperfine split component.

The Mössbauer spectra obtained at and above room temperature and given in Table 2 were all obtained under identical experi-

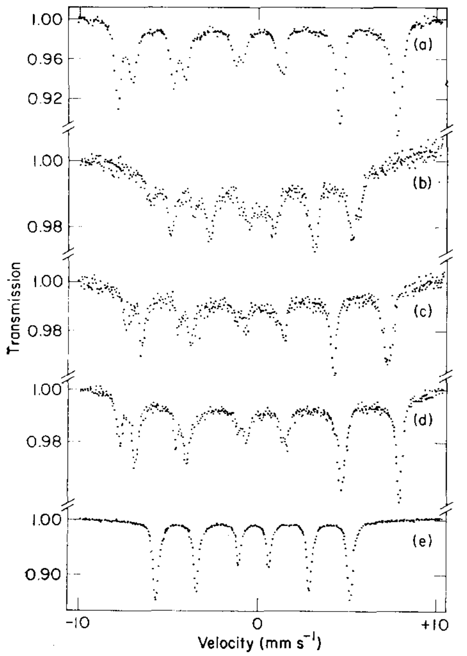

FIG. 3. Mössbauer spectra of Cr–Fe_3O_4 catalyst and a 0.001 in. Fe NBS standard foil. (a) Spectrum in air at 296 K after sample has been stored in air. (b) Sample from (a) reduced in a $CO_2/CO = 4$ mixture at 703 K for 10 hr. Spectrum obtained in reaction mixture at 703 K. (c) After cooling (b) to 483 K. (d) After cooling (c) to 296 K. (e) Spectrum of a 0.001 in. Fe NBS standard foil at 296 K.

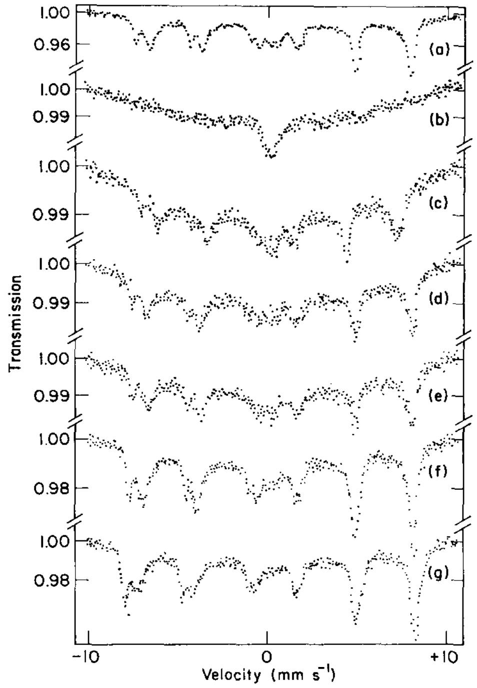

FIG. 4. Mössbauer spectra of CrPb–Fe_3O_4 catalyst. (a) Spectrum in air at 296 K after sample has been stored in air. (b) Sample from (a) exposed to a $CO_2/CO = 4$ mixture at 703 K for 12 hr. Spectrum obtained in reaction mixture at 703 K. (c) After cooling (b) to 483 K. (d) After cooling (c) to 296 K. (e) After exposing (d) to a $CO_2/CO = 4$ mixture for 14 hr. Spectrum obtained in reaction mixture at 296 K. (f) After heating (g) to 208 K. (g) Cooling (e) to 119 K in He (1 Torr).

mental conditions (Mössbauer cell, ^{57}Fe density, source-detector distance, etc.) for a meaningful comparison of the data.

Figure 7 shows Mössbauer spectra of the catalysts before and after oxidation. An α-Fe_2O_3 standard (Fig. 7g) is also included. After the first oxidation of the 7% Cr–Fe_3O_4 catalyst (Fig. 7b), the *B* spectrum disappeared completely, and the spectrum corresponded to that of γ-Fe_2O_3 with a transformation γ-$Fe_2O_3 \rightarrow \alpha$-$Fe_2O_3$, 10% to completion. The appearance of α-Fe_2O_3 is most easily seen from the shoulder on peak 5. After continued oxidation (Fig. 7c), this shoulder became even more pronounced (~30% α-Fe_2O_3), and the field reached ca. 515 kOe as for α-Fe_2O_3 or α-Fe_2O_3–Cr_2O_3 (*23*).

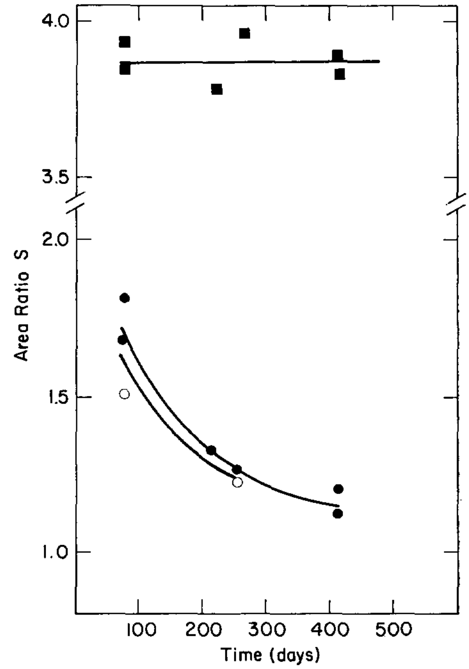

FIG. 5. The dependence of the area ratio *S* upon time exposed to air at room temperature. (○) Cr–Fe_3O_4. (●) 7% Cr–Fe_3O_4. (■) CrPb–Fe_3O_4.

After oxidation of the CrPb/Fe_3O_4 catalyst for 24 hr at 730 K, the *B* spectrum (Fig. 7e) was still present. Correspondingly, about 10% of the total O_2 uptake was taken

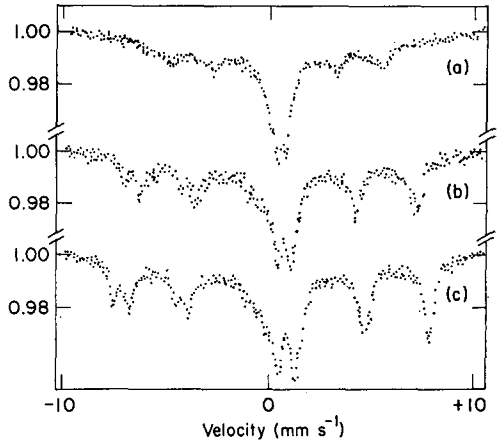

FIG. 6. Mössbauer spectra of 36% Fe_3O_4–MgO (a) 36% α-Fe_2O_3–MgO reduced in a $CO_2/CO = 4$ mixture at 703 K for 12 hr. Spectrum obtained in reaction mixture at 703 K. (b) After cooling (a) to 483 K. (c) After cooling (b) to 296 K.

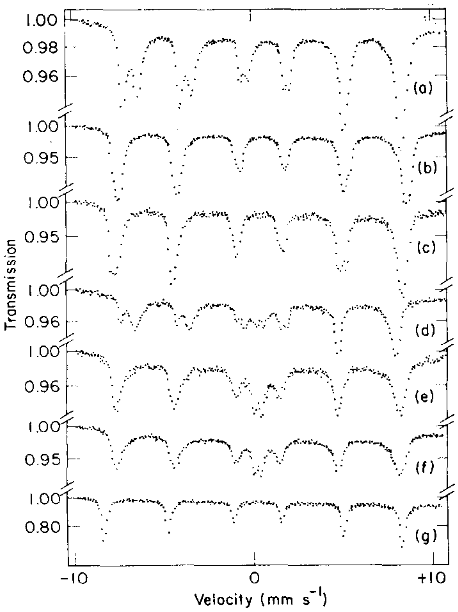

FIG. 7. Mössbauer spectra at 296 K of catalysts used for oxidation experiments. (a) 7% Cr–Fe_3O_4 after storage in air. (b) After oxidizing (a) in O_2 at 700 K for 16 hr. (c) After oxidizing (b) at 750 K for 7 hr. (d) CrPb-Fe_3O_4 catalyst after storage in air. (e) After oxidizing (d) in O_2 at 730 K for 24 hr. (f) After oxidizing (e) at 750 K for 32 hr. (g) Pure α-Fe_2O_3.

up at that stage of oxidation. By contrast, for the sample without lead, oxidation was about 95% complete after the treatment of 16 hr at 700 K.

The spectrum of the completely oxidized CrPb–Fe_3O_4 catalyst (Fig. 7f) showed, in contrast to the completely or partially oxidized 7% Cr–Fe_3O_4 catalyst, no traces of α-Fe_2O_3, and the spectrum resembled closely that of a broadened γ-Fe_2O_3 spectrum. The Mössbauer spectrum of the CrPb–Fe_3O_4 catalyst after sintering in air at temperatures above 1670 K resembled closely that of magnetite, i.e., $S \cong 2$.

Several experiments were performed to examine any possibility of synthesizing by firing techniques a lead-containing spinel with the observed Mössbauer spectrum of the CrPb–Fe_3O_4 catalyst. The Mössbauer spectra of these fired samples showed values of S around 2, and the hyperfine parameters resembled closely those of Fe_3O_4 (*13*).

DISCUSSION

Stoichiometry of Catalysts

The X ray diffraction patterns of both the Cr–Fe_3O_4 (Fig. 1a) and CrPb–Fe_3O_4 (Fig. 1b) catalysts previously exposed to air were those of single-phase stoichiometric magnetite. Addition of lead to a chromium containing catalyst does not seem to change the structure as revealed by X rays. By contrast, the Mössbauer spectra of the same catalysts without (Fig. 3a) and with (Fig. 4a) lead showed great differences, and none of them corresponded to stoichiometric magnetite (Fig. 2a). That the catalysts are not stoichiometric magnetites, as indicated by their Mössbauer spectra, was confirmed by chemical analysis since R values ($R = Fe^{3+}/Fe^{2+}$) much larger than 2 were observed. Thus, it appears that X ray diffraction is not very sensitive for detecting changes in stoichiometry or structure of substituted magnetites.

For the Cr–Fe_3O_4 catalyst exposed to air, the value of S ($S = A_{1B}/A_{1A}$) much lower than 2, and the decrease of S with increasing exposure to air at room temperature (Fig. 5), can be explained (*13*) by partial oxidation to γ-Fe_2O_3, which also has the spinel structure and can be written as $(Fe^{3+})_A[Fe_{5/3}{}^{3+}\square_{1/3}]O_4$. Both the A and B site Fe^{3+} ions in γ-Fe_2O_3 give rise to spectral components which are quite similar to the A site spectrum of Fe_3O_4. With partial oxidation, a value of R can be calculated from the observed value of S, which is in good agreement with the observed R value. As expected for an oxidized catalyst, the value of S increased after treating the Cr–Fe_3O_4 catalyst previously exposed to air with a CO–CO_2 mixture at 703 K.

The CrPb–Fe_3O_4 catalyst showed behavior quite different to that of the Cr–Fe_3O_4 catalyst. The value of S was much larger than 2 and did not change with time upon exposure to air at room temperature. The first result rules out partial oxidation to γ-Fe_2O_3, and the second finding shows that the catalyst structure is stable at room temperature, which is consistent with the fact that the CrPb–Fe_3O_4 catalyst was not oxidized as easily at high temperature as was the Cr–Fe_3O_4 catalyst. That the Mössbauer spectrum of the CrPb–Fe_3O_4 catalyst did not change after the treatment with the CO–CO_2 mixture at 703 K shows that all the experimental results obtained on the sample exposed to air are valid for the catalyst under reaction conditions.

Structure of the Cr–Fe_3O_4 Catalyst

Robbins *et al.* (*9*) have studied the $Fe_{3-x}Cr_xO_4$ system extensively. For x between 0 and 0.6, they found that S was independent of x and within experimental error equal to 2. They explained this finding by assuming that the Cr^{3+} replaced an equal amount of Fe^{3+} and Fe^{2+} on the B sites and the structure could be written as:

$$(Fe^{3+}_{1-x/2}Fe^{2+})[Fe^{3+}_{1-x/2}Fe^{2+}_{1-x/2}Cr_x^{3+}]O_4. \qquad (4)$$

The discussion of distribution of cations in spinels is facilitated by employing the parameter δ, often called the degree of inversion. The general cation distribution of the spinel $M^{2+}N_2^{3+}O_4$ can be written as:

$$(M_\delta^{2+}N^{3+}_{1-\delta})[M^{2+}_{1-\delta}N^{3+}_{1+\delta}]O_4. \qquad (5)$$

For a normal spinel $\delta = 1$, and for an inverse spinel $\delta = 0$. Thus, another way of expressing the distribution given by (4) is to say that $\delta = x/2$, i.e., the spinel does not remain completely inverted. In order to explain the value of 2 for S, Robbins *et al.* (*9*) assumed that the A site Fe^{2+} did not give rise to an observable hyperfine split spectrum due to broadening by inhomogeneous quadrupole interactions. In contrast to the findings by Robbins *et al.* we find a value of $S = 1.63$ for the Cr–Fe_3O_4 ($x = 0.15$) catalyst. This suggests that the spinel remains inverse, since the ratio S will be smaller for such a structure

$$(Fe^{3+})[Fe^{3+}_{1-x}Fe^{2+}Cr_x^{3+}]O_4. \qquad (6)$$

However, after the Cr–Fe_3O_4 catalyst is sintered at 1040 K in a CO–CO_2 mixture the value of S becomes equal to 2 as observed by Robbins *et al.* (*9*). In this system, equilibrium site distribution should be independent of prior heat treatment, since only electron transfer is required to change from structure (5) to structure (6). This suggests that the equilibrium cation distribution may depend on particle size. Thus the Cr–Fe_3O_4 catalyst may have a structure quite different from the corresponding bulk structure.

Structure of the CrPb–Fe_3O_4 Catalyst

For the CrPb–Fe_3O_4 catalyst, we observed $S \cong 4$. The high value does not indicate *a priori* in which site the lead is present. Since only 5% lead is present, it follows that a "simple" substitution of lead on either the A or the B site would not result in such a drastic change on S. Further, S stays practically constant over the temperature range studied. Thus, the large value of S cannot be explained by a large change in the recoil free fractions.

An analysis of S is difficult because we do not know whether all the cations contribute to the resolved spectra, since some of the cations may have large distributions in the magnetic and quadrupole interaction and will give rise to a broad spectrum contributing to the background count rate. Thus, the total background-corrected spectral areas per ^{57}Fe atom were measured for samples with and without lead and were found to be between 0 and 20% lower for the lead-containing catalysts. Therefore, the spectral contribution of a major fraction of the iron atoms does not appear to be lost in the background.

The Mössbauer spectrum of the CrPb–Fe_3O_4 catalyst showed the presence of a paramagnetic doublet. From the spectra taken at different temperatures, it is clear that this doublet is not indicative of a separate phase but rather of superparamagnetic behavior (*13*). A comparison of the superparamagnetic behavior of the CrPb–Fe_3O_4 catalyst with that of the smaller Fe_3O_4 particles in the 36% Fe_3O_4–MgO catalyst indicates that the CrPb–Fe_3O_4 exhibits superparamagnetic clusters, the size of which is much smaller than the particle size. This behavior is similar to that described by Raj and Kulshreshtha for the Li–Al (*24*) and Ni–Zn (*25*) ferrite systems.

In the next sections the Mössbauer parameters will be analyzed in detail in order to obtain structural information about the CrPb–Fe_3O_4 catalyst. It will be assumed that the spinel structure is maintained, and, indeed, no nonspinel Mössbauer or X ray phases were detected. The analysis of the Mössbauer parameters led to the proposal of a model for the structure of the catalyst. For the sake of clarity the model will be presented before the results upon which it is based. The model has the following characteristics:

M1. Lead is present as Pb^{4+}.

M2. Pb^{4+} enters the tetrahedral A site.

M3. The A sites expand and the B sites contract.

M4. The spinel structure becomes partly normal.

M5. Some Fe^{2+} is oxidized according to Eq. (1).

The above characteristics will be denoted as (M1), (M2), etc., which will be used subsequently when information supporting the corresponding characteristic of the model is given.

Linewidth. An analysis of the linewidth is helpful, since information about electron hopping times and homogeneity of the cation surroundings can be obtained. For Fe_3O_4 a temperature independent linewidth of the $1A$ line, Γ_{1A}, is observed. As the temperature is lowered, Γ_{1B} increases according to the decreased rate of electron hopping; the electron hopping time at room temperature is found to be around 1 ns, in agreement with literature values (*26, 27*).

For the catalyst containing lead, we observe, as we did for Fe_3O_4, a narrow and temperature-independent linewidth for the $1A$ line. This indicates that the A site of iron does not seem to have any nonmagnetic B site neighbors, indicating that lead does not enter the B site (M2).

The linewidth of the B site is very large at all temperatures as compared to the corresponding value for the Fe_3O_4 sample. The low temperature behavior shows that the electron hopping has slowed down in the CrPb–Fe_3O_4 catalyst as compared to pure Fe_3O_4. The large linewidths at higher temperatures indicate that the B site iron atoms have a distribution in magnetic interactions caused by the presence of lead in the A site. The broadening of the $1B$ line at higher temperatures could be due to a distribution in exchange interactions and also to a distribution in superparamagnetic transition temperatures. From a comparison of the CrPb–Fe_3O_4 and 36% Fe_3O_4–MgO results, we see that the broadening cannot be explained only by the particle size effect. Thus, the situation where lead is present in the A site seems to account for the broadening observed (M2).

Hyperfine fields. A meaningful analysis of the hyperfine fields is somewhat complicated by the fact that there exists a particle size distribution. Such a distribution will lower the observed fields and give rise to an apparent lowering in the Néel temperature. In order to eliminate changes in the hyperfine fields caused by changes in Néel temperature, Babeshkin *et al.* (*28*) used the behavior of H vs T/T_N, where T_N is the Néel temperature, to determine in which site Sc^{3+} enters $MnFe_2O_4$. The magnetic field depends on the number of magnetic neighbors, and since the H_B vs T/T_N data for the Sc^{3+}-substituted $MnFe_2O_4$ superimposed on the H_B vs T/T_N data for pure $MnFe_2O_4$, it was concluded that Sc^{3+} enters the B site. By using the Mössbauer results for the $Zn_xFe_{3-x}O_4$ obtained by Dobson *et al.* (*20*), we are able to show that the above type of arguments are also valid for substitutions of nonmagnetic ions into the A sites (*13*). In order to analyze the hyperfine fields for the CrPb–Fe_3O_4 catalyst, a value of T_N must be chosen. The choice of T_N is not easy, since the catalyst consists of small particles. In order to take care of particle size complication, it was decided to compare the hyperfine fields for the CrPb–Fe_3O_4 catalyst with those of the 36% Fe_3O_4–MgO catalyst, since these two catalysts exhibit quite similar superparamagnetic behavior. The hyperfine field data for the two catalysts are shown in Fig. 8. We observe a close agreement between the A site magnetic fields for the two catalysts, whereas the B site magnetic fields for the lead-containing catalyst is somewhat lower. This shows that the exchange interactions of the B site cations have been lowered, indicating that the lead must be located at the tetrahedral sites (M2).

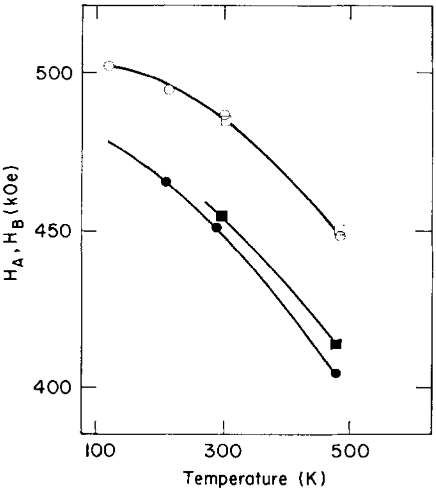

FIG. 8. Temperature dependence of hyperfine fields. (○) H_A for CrPb-Fe_3O_4. (□) H_A for 36% Fe_3O_4-MgO. (■) H_B for 36% Fe_3O_4-MgO. (●) H_B for CrPb-Fe_3O_4.

Isomer shift. An analysis of the isomer shift gives information about the electron density at the nucleus. The isomer shifts at temperatures equal to or below room temperature of the A site, $\delta_{A,Fe}$, is larger for the CrPb-Fe_3O_4 catalyst than for the Fe_3O_4 sample. The decrease in the electron density at the nucleus of the A sites for the lead-containing catalyst is indicative of a decrease in covalency caused by an expansion of the A site (M2 and M3). The temperature derivative of the isomer shift $\Delta\delta/\Delta T$ increases when the mean square displacement of the resonating atom increases. We would expect an increase in $\Delta\delta_A/\Delta T$ if the A site expands, and this is indeed observed (M3). The radii r_A and r_B of spheres inscribed in the A and B sites, respectively, can be given by [see (*8*)]:

$$r_A = (u - 1/4)a3^{1/2} - R_O \qquad (7)$$

$$r_B = (5/8 - u)a - R_O \qquad (8)$$

where a is the lattice parameter, R_O is the radius of the oxygen ion, and u is the oxygen parameter. For the ideal fcc oxygen lattice u is 3/8. For $u > 3/8$, Verwey *et al.* (*29*) showed that the normal configuration has the larger Madelung constant and is more stable than the inverse configuration.

The above results showed an increase in r_A. If this increase is due to a lattice expansion and not to an increase in u, we would expect that the B site has also expanded. The X ray diffraction studies showed slight increase in the lattice constant for lead-containing catalysts. However, this observed lattice expansion can only explain a negligible increase in r_A, and, thus, an increase in u must account for the increase in r_A. Hence, it follows that the radius of the B site must decrease, and this is clearly indicated by the decrease in $\Delta\delta_B/\Delta T$ (M3). From Mössbauer spectroscopy only information concerning the iron cations is obtained. From the above results, it appears that, when lead is present, a structure with a larger value of u is formed (M3). In this structure the sizes of all the tetrahedral and octahedral sites have expanded and contracted, respectively, in relation to the sites in magnetite (M3). The decrease in the mean-square displacement of the B cations should also show up as an increase in the recoil-free fraction, f_B, of the B site cations. When the Mössbauer spectral areas are plotted versus the temperature, we observe a smaller decrease in the areas, as the temperature increases for the spectra of the lead-containing catalyst than for those of the lead-free catalyst. Thus, f_B of the lead-containing catalyst is larger than that of the lead-free catalyst (M3).

The CrPb-Fe_3O_4 catalyst did not show any $\gamma \rightarrow \alpha$-$Fe_2O_3$ transition. As shown by deBoer and Selwood (*30*), substituting a small ion like Al^{3+} into the B site of γ-Fe_2O_3 stabilizes γ-Fe_2O_3 toward the $\gamma \rightarrow \alpha$-$Fe_2O_3$ transition. Thus, the stabilization of the γ-Fe_2O_3 structure for lead-containing catalysts observed by X ray diffraction and Mössbauer spectroscopy is consistent with (M2) and (M3).

Quadrupole splitting and S and R ratios. When the tetrahedral site expands it is usually assumed that the A-site cubic symmetry with respect to its four surrounding oxygen ions is retained (*8*). As a result, the oxygens surrounding each B ion no longer have cubic symmetry. The quadrupole splitting observed by Mössbauer spectroscopy depends on the electrical field gradient at the nucleus. Consequently, changes in quadrupole splitting will be expected when changes in symmetry of the iron ions occur. When combined magnetic and quadrupole interactions are present and the electrical field gradient tensor is axially symmetric, the perturbation, ϵ, of each of the excited magnetically split levels is given by

$$\epsilon = e^2qQ(3\cos^2\theta - 1)/8 \qquad (9)$$

where ϵ is the charge of the proton, Q is the quadrupole moment of the nucleus, $eq = V_{zz}$ is the maximum value of the field gradient, and θ is the angle between the principal axis of the electric field gradient tensor and the magnetic axis.

For the CrPb–Fe_3O_4 catalyst, values of ϵ_A are quite close to the corresponding values for the lead-free samples. In contrast, the values of ϵ_B for the lead-containing catalyst are notably different from the values of ϵ_B obtained for all other samples. These results suggest that for the lead-containing catalyst the B sites, but not the A sites, change symmetry upon lead substitution (M2).

The value of ϵ_B for the CrPb–Fe_3O_4 catalyst is smaller than that of Fe_3O_4. Comparing this result with the ϵ_B data of Dobson *et al.* (*20*) on the $Zn_xFe_{3-x}O_4$ system, where ϵ_B was shown to decrease with increasing x, also indicates that Pb enters the tetrahedral sites.

So far we have not discussed in detail in what valence state the lead is present. From the chemical analysis data given in Table 1, Pb^{4+} satisfies the charge balance better than Pb^{2+} (M1). Also it seems very unlikely that the large Pb^{2+} ion ($r = 1.2$ Å) could be present on either the A- or the B-site, and it is more likely that the lead is present as Pb^{4+} ($r = 0.84$ Å) (M1).

Now we will deal with the large observed value of S for the lead-containing catalyst. Let us first consider the structure of a chromium-containing catalyst in its most general form,

$$(Fe_\delta{}^{2+}Fe^{3+}{}_{1-\delta})[Fe^{3+}{}_{1+\delta-y}Cr_y{}^{3+}Fe^{2+}{}_{1-\delta}]O_4. \qquad (10)$$

Assume that Pb^{4+} enters this structure according to the replacement reaction symbolized by

$$2Fe^{2+} \rightarrow \square + Pb^{4+}. \qquad (11)$$

Then, the structure becomes,

$$(Pb_x{}^{4+}\square_xFe^{2+}{}_{\delta-2x}Fe^{3+}{}_{1-\delta})[Fe^{3+}{}_{1+\delta-y}Cr_y{}^{3+}Fe^{2+}{}_{1-\delta}]O_4. \qquad (12)$$

In the case of the CrPb–Fe_3O_4 catalyst, x and y are known, and only δ remains unknown.

Large values of S can now easily be understood in terms of the structure (*12*). The A site $Fe_{\delta-x}{}^{2+}$ does not show a spectral pattern and is most likely lost in the background (*9*). A low values of $\delta_{B,\mathrm{Fe}}$ is observed for the lead-containing catalyst. This could indicate that the electron hopping occurs between octahedral ions rich in Fe^{3+}; thus the observed B pattern seems to be caused by all the B ions. The area ratio can now be expressed as

$$S = (2 - y)/(1 - \delta). \qquad (13)$$

Since y is small, values of δ (only δ's with subscript refer to isomer shifts) around 0.5 can explain the observed value of S (M4). This value of δ is the value of δ for a $Zn_xFe_{3-x}O_4$ sample having the same value of ϵ_B as the CrPb–Fe_3O_4 catalyst.

From Eq. (12) a value of $R = 2.64$, independent of δ, would be expected. This is somewhat smaller than the observed R. Derbyshire and Yearian (*31*) showed that in the $Cr_xFe_{3-x}O_4$ spinel system the difference between the mean ionic size of the B site ion and the size of the B site (calculated from u, a, and R_O using Eq. (8) stayed constant. Thus, in the CrPb–Fe_3O_4 structure, where the size of the B site has decreased, there might be a tendency toward a decrease in the mean ionic size of the B site cations. One possible way this decrease can be accomplished is by oxidizing some of the Fe^{2+} ions in the B site according to Eq. (1). If we consider this possibility (*13*), consistency between both the observed R and S ratios are obtained (M5).

Active Solid Nature of the Catalyst Structures

Upon sintering the CrPb–Fe_3O_4 catalyst the structure changes completely, and by X ray diffraction we observe the exclusion of the lead from the magnetite phase. The Mössbauer spectra become after thorough sintering similar to that of Cr–Fe_3O_4 (i.e., $S \cong 2$). Thus the structure of the CrPb–Fe_3O_4 catalyst appears to be metastable, but the structure is stable under reaction conditions.

The Mössbauer parameters of magnetites with and without lead prepared by firing in vacuum at high temperatures showed that lead does not affect the hyperfine parameters to any great extent. It is known that the degree of inversion of a spinel can depend on the thermal history, such as the quenching temperature (*8*). Treating the fired CrPb–Fe_3O_4 samples in a CO–CO_2 mixture at 703 K does not, however, change the Mössbauer spectrum into that of the lead-containing catalyst; rather the spectrum resembles that of the sintered Cr–Fe_3O_4 catalyst. It must, therefore, be concluded that, under usual ceramic methods of preparation, lead does not enter to any appreciable extent into magnetites. These results also suggest that the structure of the catalyst is metastable and that the structure might be denoted as an "active solid." Fricke gives three reasons why catalysts might be active solids (i.e., solids with excess free energy) (*32*). These reasons are: (1) solids with large surface to volume ratio, (2) solids containing defects, and (3) solids having "memory" due to the method of preparations. The particle size of the catalysts studied here is above the region where the surface is expected to be important in determining the structure. However, in the case of the Cr–Fe_3O_4 catalyst, there does not seem to be an equal number of Fe^{2+} and Fe^{3+} cations on the octahedral sites as is the case of the bulk spinel. This equality of number was argued by Robbins *et al.* (*9*) to be favorable due to the electron hopping. As the particle size of Fe_3O_4 is decreased, a decrease in the electron hopping time is observed (*13*). This may explain why a different structure for the Cr–Fe_3O_4 catalyst is observed. The method of preparation has probably also been a determining factor in the resulting active solids, and it is not surprising that a metastable structure arises from a wet preparation procedure, but that these structures are stable under reaction condition shows that the active solids have catalytic interest and their structure must be considered when describing the nature of the catalytic action.

CONCLUDING REMARKS

Finally, some speculations on the nature of the increased activity of the CrPb–Fe_3O_4 catalyst may be offered. Several investigations (*33–35*) have mentioned the importance of the degree of covalency of the metal oxygen bond and electron transfer in oxidation reactions. Boreskov (*35*) reports that the electron transfer is facilitated by an increase in the covalent character of the metal oxygen bond. Schwab *et al.* (*36*) investigated the oxidation of CO on ferrites and found that the activity could be correlated with the octahedral ions. Since the CrPb–Fe_3O_4 catalyst showed increased covalency of octahedral ions, this could explain the increased activity toward the CO conversion.

ACKNOWLEDGMENTS

We are deeply grateful to Hans Bohlbro not only for supplying the catalyst samples which prompted this work but also for many stimulating discussions. This investigation was supported by NSF Grant GK 17451X with help from the Center for Materials Research at Stanford University. The collaboration of Calvin Bartholomew in the early stages and of James Dumesic in the latter stages of the work is also acknowledged.

REFERENCES

1. BOHLBRO, H., "An Investigation on the Kinetics of the Conversion of Carbon Monoxide with Water Vapour Over Iron Oxide Based Catalysis," Gjellerup, Copenhagen, 1966.

2. TOPSØE, H. F. A., Ger. Offen. 2,009,374 (1970).

3. BOHLBRO, H., private communication.

4. GORTER, E. W., *Phillips Res. Rep.* **9**, 295 (1954).

5. MAZANEK, E. S., JASIENSKA, S., AND WYDERKO, M. E., Modern Blast Furn. Conf. Proc., Cracow, 1965.

6. DRY, M. E., AND FERREIRA, L. C., *J. Catal.* **6**, 194 (1966).

7. HRYNKIEWICZ, A. Z., KULGAWCZUK, D. S., MAZANEK, E. S., PUSTOWKA, A. J., SAWICKI,

J. A., AND WYDERKO, M. E., *Phys. Status Solidi* **43**(b), 401 (1971).

8. SMIT, J., AND WIJN, H. P. J., "Ferrites," Wiley, New York, 1959.
9. ROBBINS, M., WERTHEIM, G. K., SHERWOOD, R. C., AND BUCHANAN, D. N. E., *J. Phys. Chem. Solids* **32**, 717 (1971).
10. ZINN, W., HÜFNER, S., KALVIUS, M., KIENLE, P., AND WIEDEMANN, W., *Z. Angew. Physik* **17**, 147 (1964).
11. KHAMMOUMA, S., Ph.D. Dissertation, Stanford University, 1972.
12. BARTHOLOMEW, C., AND BOUDART, M., *J. Catal.* **29**, 278 (1973).
13. TOPSØE, H., Ph.D. Dissertation, Stanford University, 1972.
14. SPIJKERMAN, J. J., DEVOE, J. R., AND TRAVIS, J. C., NBS Special Report 260-20, May 1970.
15. BARTHOLOMEW, C., Ph.D. Dissertation, Stanford University, 1972.
16. KLUG, H. P., AND ALEXANDER, L. E., "X-ray Diffraction Procedures," Chap. 9. Wiley, New York, 1967.
17. ARMSTRONG, R. J., MORRISH, A. H., AND SAWATZKY, G. A., *Phys. Letters* **23**, 415 (1966).
18. KÜNDIG, W., *Bull. Amer. Phys. Soc.* **13**, 667 (1968).
19. SAWATZKY, G. A., VAN DER WOUDE, F., AND MORRISH, A. H., *Phys. Rev.* **183**, 383 (1969).
20. DOBSON, D. D., LINNETT, J. W., AND RAHMAN, M. M., *J. Phys. Chem. Solids* **31**, 2727 (1970).
21. VAN DER WOUDE, F., SAWATZKY, G. A., AND MORRISH, A. H., *Phys. Rev.* **167**, 533 (1968).
22. BANERJEE, S. K., O'REILLY, W., AND JOHNSON C. E., *J. Appl. Phys.* **38**, 1289 (1967).
23. SHIRANE, G., COX, D. E., AND RUBY, S. L., *Phys. Rev.* **125**, 1158 (1962).
24. RAJ, P., AND KULSHRESHTHA, S. K., *J. Phys. Chem. Solids* **31**, 9 (1970).
25. RAJ, P., AND KULSHRESHTHA, S. K., *Phys. Status Solidi* 4(a), 501 (1971).
26. KÜNDIG, W., AND HARGROVE, R. S., *Solid State Commun.* **7**, 223 (1969).
27. SAWATSKY, G. A., COEY, J. M. D., AND MORRISH, A. H., *J. Appl. Phys.* **40**, 1402 (1969).
28. BABESHKIN, A. M., POCHOLOK, K. V., YERSHOVA, Z. P., PERFILEO, D. YU., POKROVSKY, I. B., AND KOMISSAROVA, L. N., "Proc. of the Conf. on the Application of the Mössbauer Effect, Tihany, Hungary (1969)" (I. Dezi, Ed.), p. 541. Adakemiai Kiado, Budapest, 1971.
29. VERWEY, E. J. W., AND HEILMANN, E. L., *J. Chem. Phys.* **15**, 174 (1947).
30. DEBOER, F. E., AND SELWOOD, P. W., *J. Amer. Chem. Soc.* **76**, 3365 (1954).
31. DERBYSHIRE, W. E., AND YEARIAN, H. J., *Phys. Rev.* **112**, 163 (1958).
32. FRICKE, R., *Naturwissenschaften* **31**, 469 (1943).
33. CIMINO, A., AND SCHIAVELLO, M., *J. Catal.* **20**, 202 (1971).
34. CIMINO, A., PEPE, F., AND SCHIAVELLO, M., "Fifth International Congress on Catalysis," North-Holland, Amsterdam, 1972. (Preprint No. 1.)
35. BORESKOV, G. K., *ibid.* (Preprint No. 71.)
36. SCHWAB, G. M., ROTH, E., GRINTZOS, CH., AND MAVRAKIS, N., "Structure and Properties of Solid Surfaces," (R. C. Gomer and C. S. Schmidt, Eds.), p. 464. The University of Chicago Press, Chicago, 1953.